

Supporting Information

Effects of Morphology and Temperature on the Tensile Characteristics of Carbon Nitride

Nanothreads

Yuequn Fu,^a Ke Xu,^b Jianyang Wu,^{*ab} Zhiliang Zhang^a and Jianying He^{*a}

^aNTNU Nanomechanical Lab, Norwegian University of Science and Technology (NTNU), Trondheim
7491, Norway

^bDepartment of Physics, Research Institute for Biomimetics and Soft Matter, Jiujiang Research Institute
and Fujian Provincial Key Laboratory for Soft Functional Materials Research, Xiamen University,
Xiamen 361005, PR China

*Corresponding Emails: jianyang@xmu.edu.cn, jianying.he@ntnu.no

For verification of the ReaxFF forcefield, tensile mechanical properties of a selected CNNT of IV-7 were computed by DFT calculations, as implemented in VASP (Vienna Ab initio Simulation Package) code¹. The projector augmented wave (PAW) method was utilized to describe the ion-electron interaction in the CNNT. The generalized gradient approximation (GGA) with Perdew-Burke-Ernzernh (PBE) exchange correlation function² was used with a kinetic energy cutoff of 650 eV. Dimensions of $25 \times 25 \text{ \AA}^2$ in the transverse directions was created to avoid spurious interactions as a result of the application of PBC. The first Brillouin zone was sampled using a $1 \times 1 \times 15$ Monkhorst-Pack mesh. At each stretching step, atomic positions in the structure were fully relaxed with fixing axial dimension of the simulation box until an energy convergence of 10–5 eV and a force convergence of 0.01 eV/ \AA were reached. It is revealed that both DFT and ReaxFF-based MD simulations predicted similar Young's modulus, failure strain and brittle fracture (Figure S1), indicating the reasonable application of ReaxFF forcefield for predicting tensile mechanical characteristics of CNNTs.

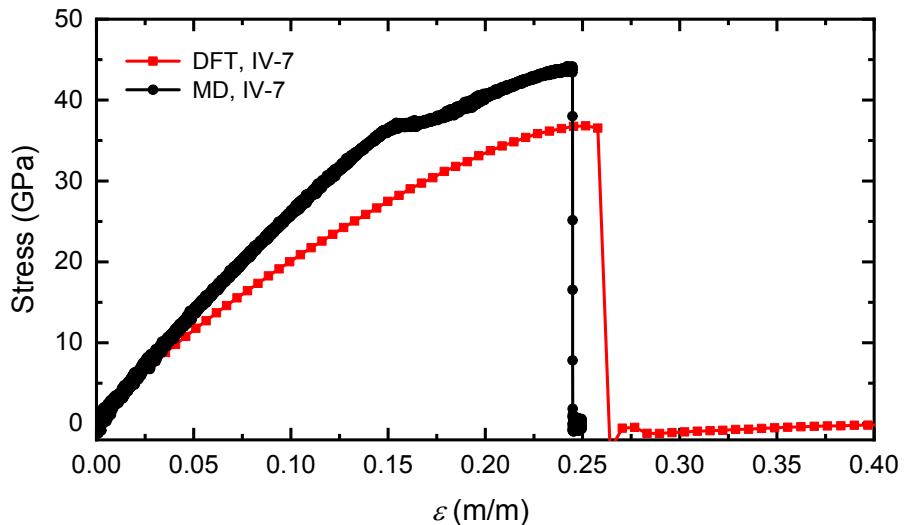


Figure S1 Comparison of global tensile stress-strain curves of selected IV-7 CNNT by DFT and ReaxFF-based MD calculations.

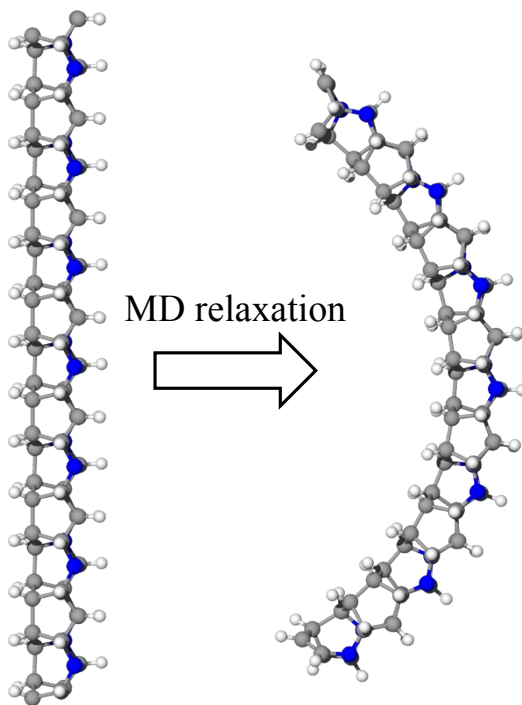


Figure S2 Configurational motif of a segment of Zipper polymer_24 after fully MD relaxiation.

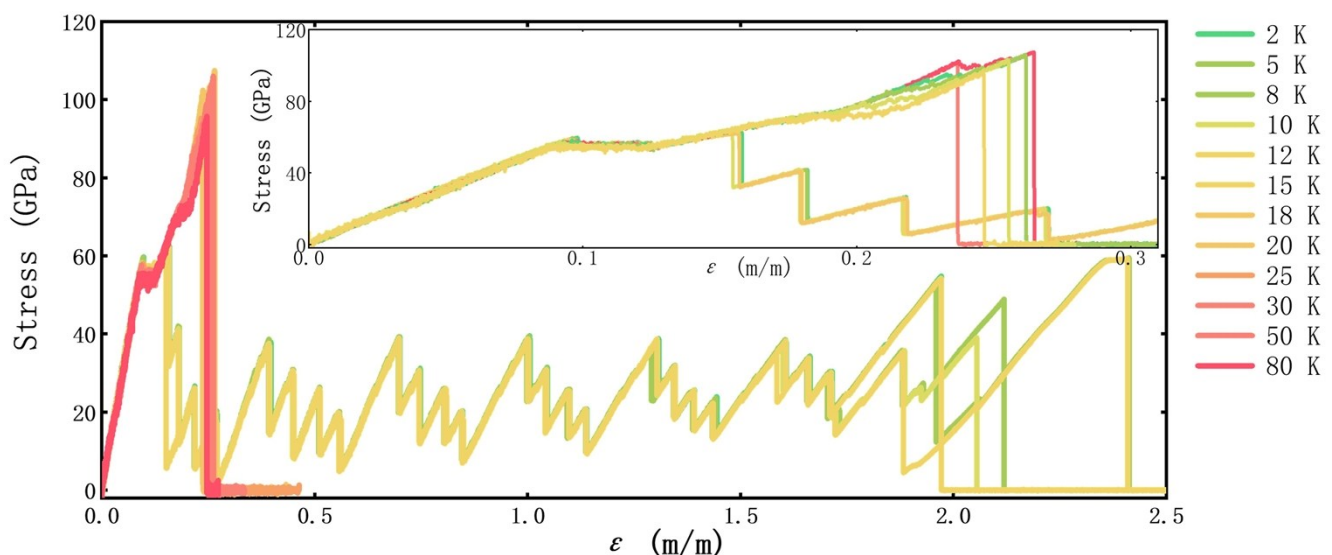


Figure S3 Mechanical performance of Polymer I_3-3_25 CNNT under temperature ranging from 2-80 K.

The insert shows the stress-strain curves at small scale deformation.

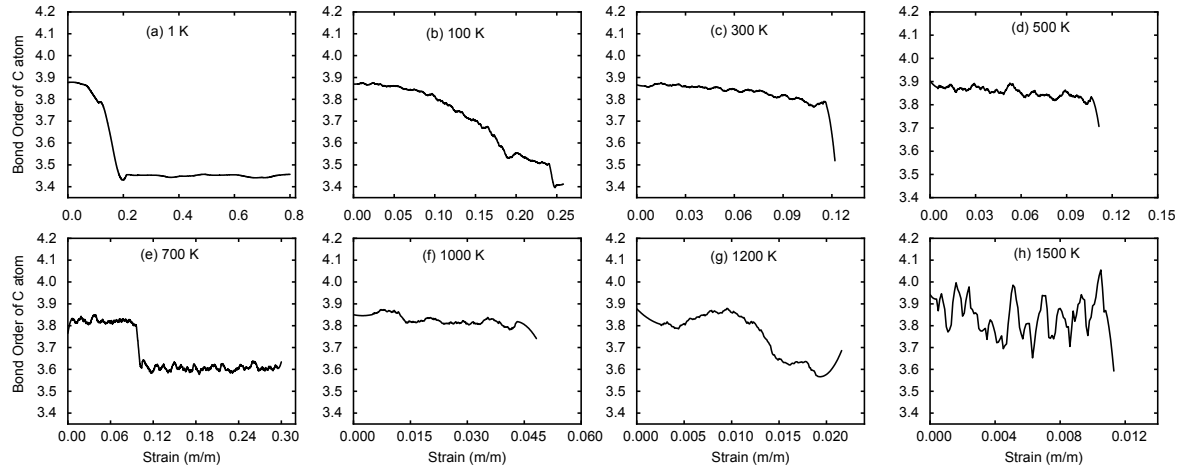


Figure S4 (a)-(h) Variation in the chemical BOs of one carbon atom with globally axial strain for Polymer I_3-3_25 at temperature from 1-1500 K, respectively.

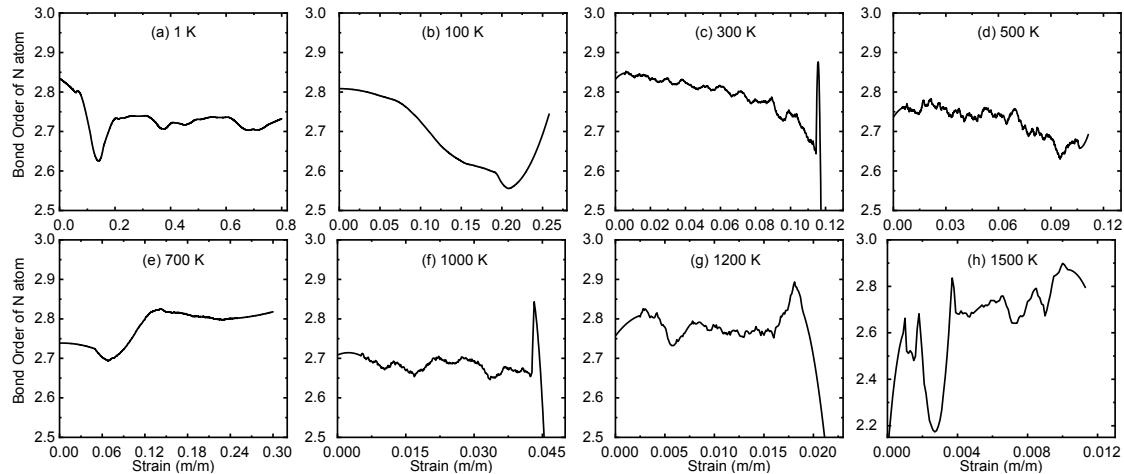


Figure S5 (a)-(h) Variation in the chemical BOs of one nitrogen atom with globally axial strain for Polymer I_3-3_25 at temperature from 1-1500 K, respectively.

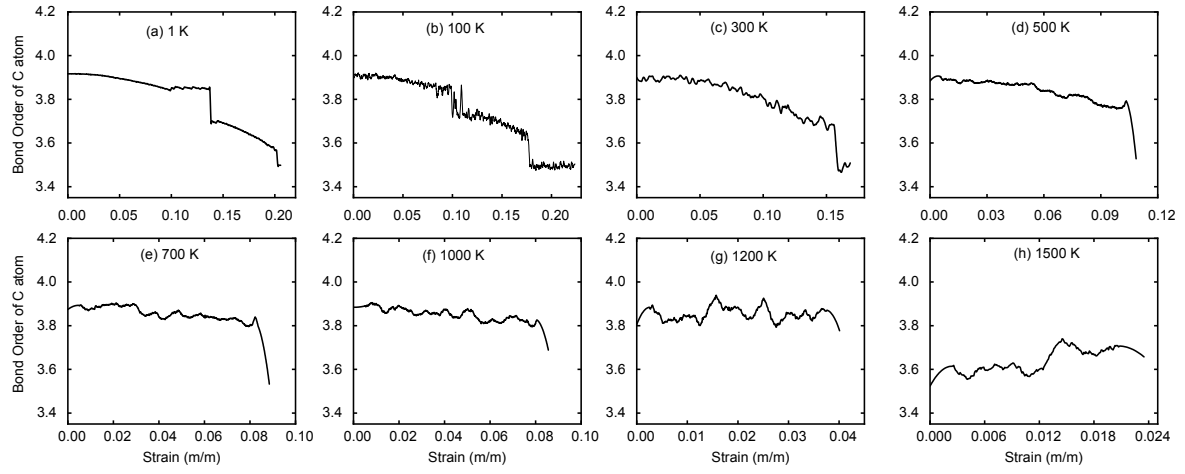


Figure S6 (a)-(h) Variation in the chemical BOs of one carbon atom with globally axial strain for Polymer I_4-2_36 at temperature from 1-1500 K, respectively.

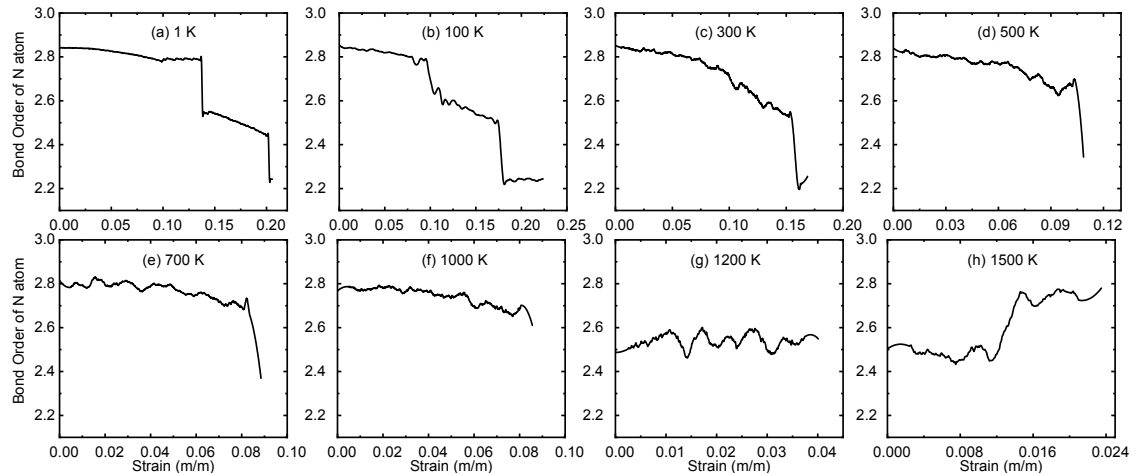


Figure S7 (a)-(h) Variation in the chemical BOs of one nitrogen atom with globally axial strain for Polymer I_4-2_36 at temperature from 1-1500 K, respectively.

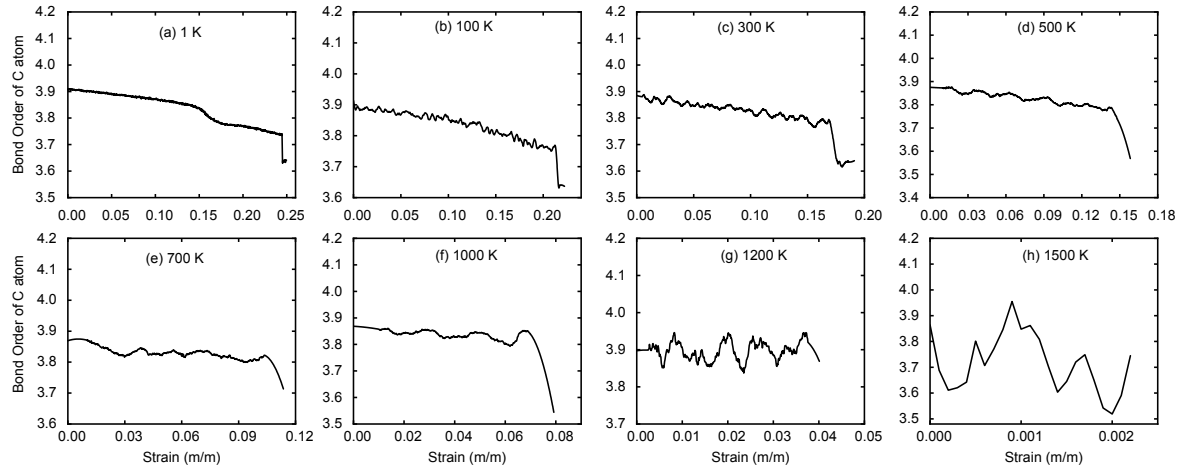


Figure S8 (a)-(h) Variation in the chemical BOs of one carbon atom with globally axial strain for IV-7 at temperature from 1-1500 K, respectively.

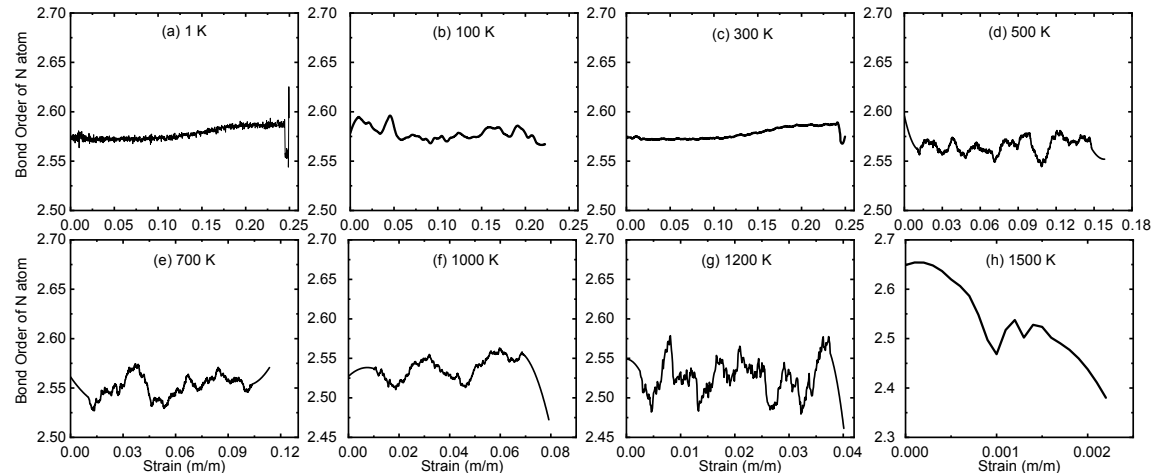


Figure S9 (a)-(h) Variation in the chemical BOs of one nitrogen atom with globally axial strain for IV-7 at temperature from 1-1500 K, respectively.

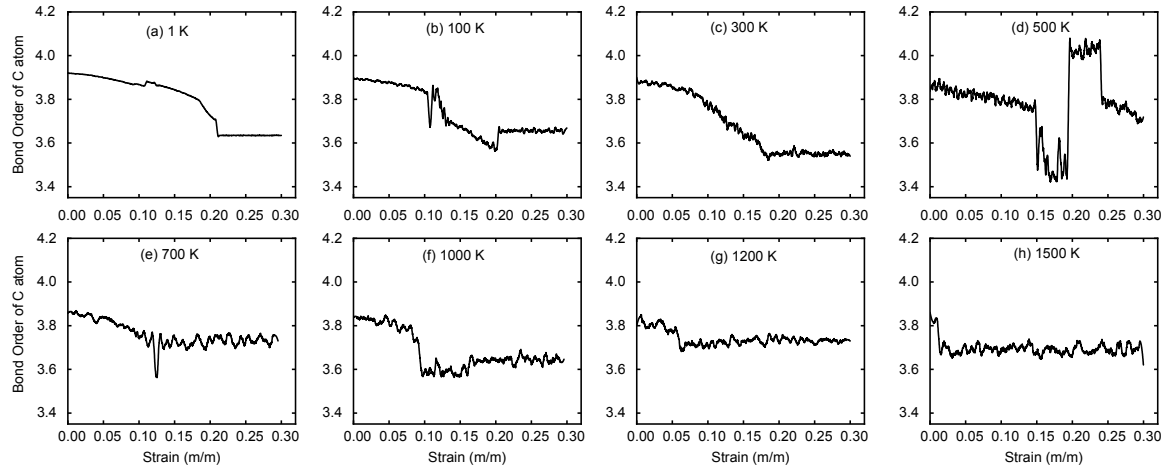


Figure S10 (a)-(h) Variation in the chemical BOs of one carbon atom with globally axial strain for Polytwistane_153 at temperature from 1-1500 K, respectively.

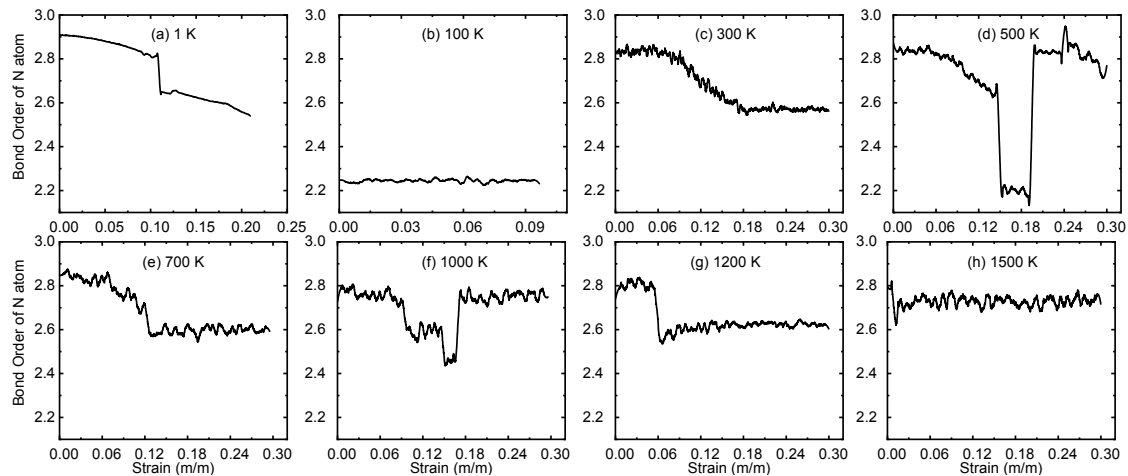


Figure S11 (a)-(h) Variation in the chemical BOs of one nitrogen atom with globally axial strain for Polytwistane_153 at temperature from 1-1500 K, respectively.

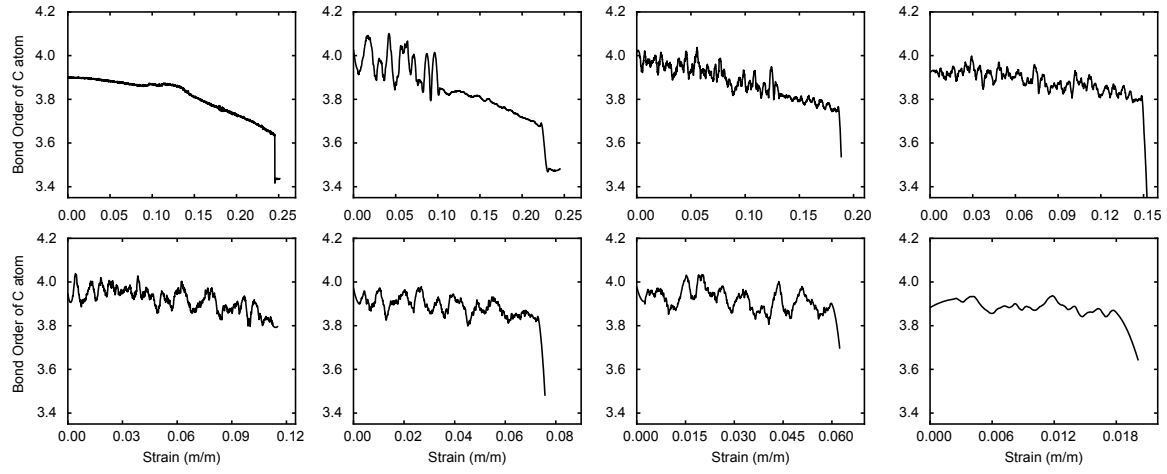


Figure S12 (a)-(h) Variation in the chemical BOs of one carbon atom with globally axial strain for Tube (3,0)_123456 at temperature from 1-1500 K, respectively.

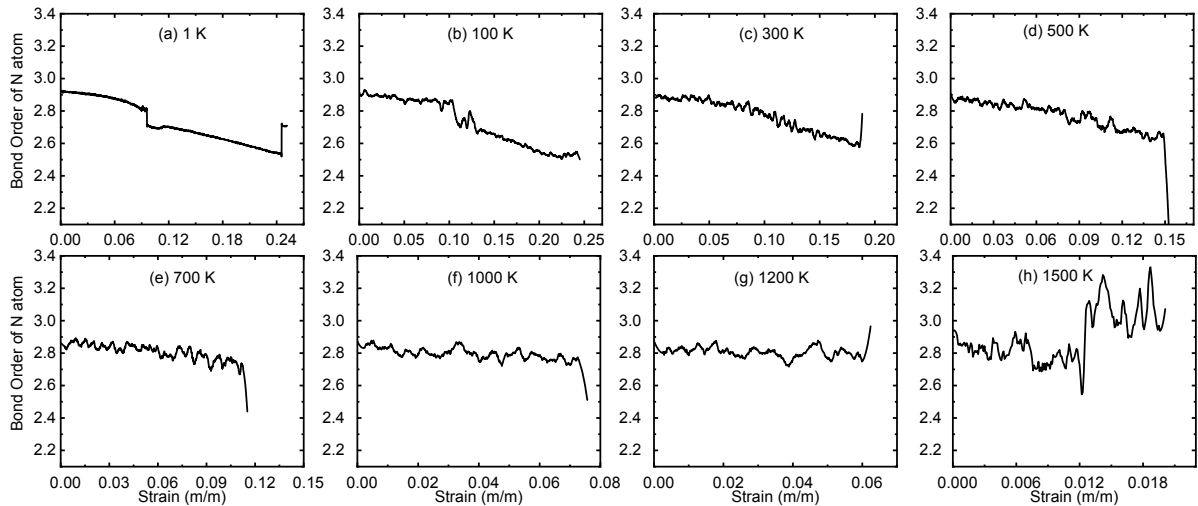


Figure S13 (a)-(h) Variation in the chemical BOs of one nitrogen atom with globally axial strain for Tube (3,0)_123456 at temperature from 1-1500 K, respectively.

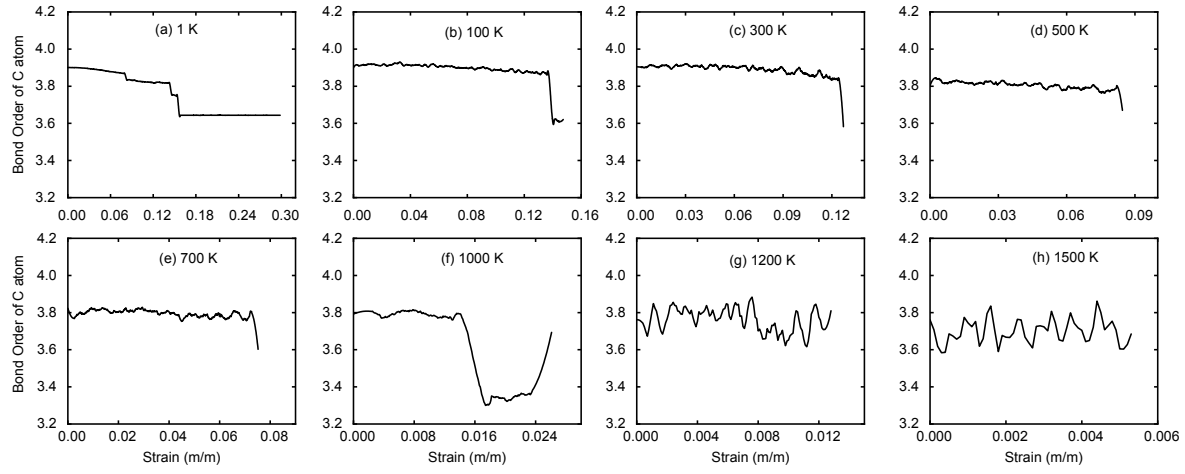


Figure S14 (a)-(h) Variation in the chemical BOs of one carbon atom with globally axial strain for Zipper polymer_24 at temperature from 1-1500 K, respectively.

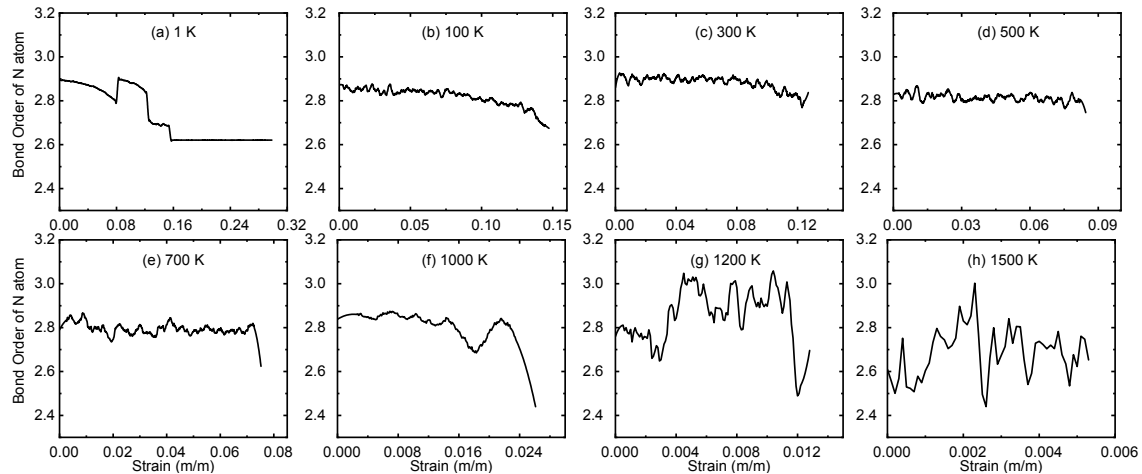


Figure S15 (a)-(h) Variation in the chemical BOs of one nitrogen atom with globally axial strain for Zipper polymer_24 at temperature from 1-1500 K, respectively.

Dynamics of Bond Length in CNNTs

Failure of CNNTs by axial elongation is mainly characterized by deformation-induced dissociation of localized covalent bonds. Elongation development of localized bonds is therefore monitored to

understand the deformation mechanisms. Figure S16 shows the relationships of bond length-strain in the skeleton of relatively weak IV-7 under axial extension at different temperatures. Clearly, the bond length in IV-7 CNNT changes with increasing strain. At low temperatures (1-300 K), strong nonlinearity in the bond length-strain curves is identified, explaining its nonlinear elasticity as illustrated in Figure 8c. Moreover, there is a critical strain after which change in bond length becomes more pronounced as the strain is further applied. The critical strain corresponds to the slightly mechanical softening of IV-7 CNNT in Figure 8c. At high temperatures, however, the bond is almost linearly lengthened with increasing axial strain. Moreover, elongation in bond length becomes less significant with increasing axial strain. As the axial is applied to a critical value, bond length jumps because of tension induced dissociation of the bond. Figure S17 plots the variation in the bond length with global strain for mechanically robust Tube (3,0)_1245 CNNT at different temperatures. Similarly, covalent bond in the skeleton is strongly nonlinearly elongated with increasing axial strain at low temperatures. However, there are two critical strains in critical changes of bond length; Increase in the bond length becomes more pronounced as the elongation is overstrain of around 0.075, but then becomes less significant when the applied strain is over about 0.12. Such “S”-shaped curve of bond length-strain is able to explain the unique mechanical loading curve of Tube (3,0)_1245 CNNT where an initial softening but then a stiffening appears. At high temperature, the bond length is almost linearly increased with increasing axial strain, and the elongation in bond length becomes less pronounced as the axial strain is increased. Furthermore, it is observed that, at low temperatures, the bond dissociates once the bond length is over around 1.8 Å, whereas, at high temperatures, the bond is broken as the bond length below 1.8 Å. With regard to other CNNTs, it is similarly found that the bond length nonlinearly increases with increasing strain at low temperatures, whereas at high temperatures the localized bond is linearly elongated as the global axial strain is applied, as shown in Figure S18-S22.

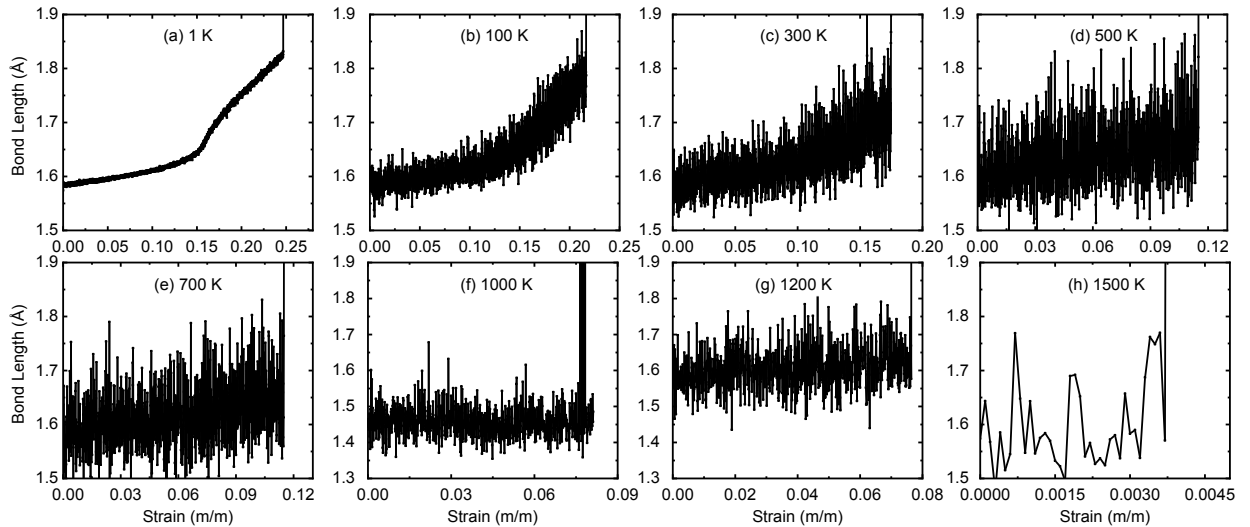


Figure S16 Development of bond length of the skeleton under tension. (a)-(h) Variation in a localized bond length with globally axial strain for IV-7 at temperature ranging from 1-1500 K.

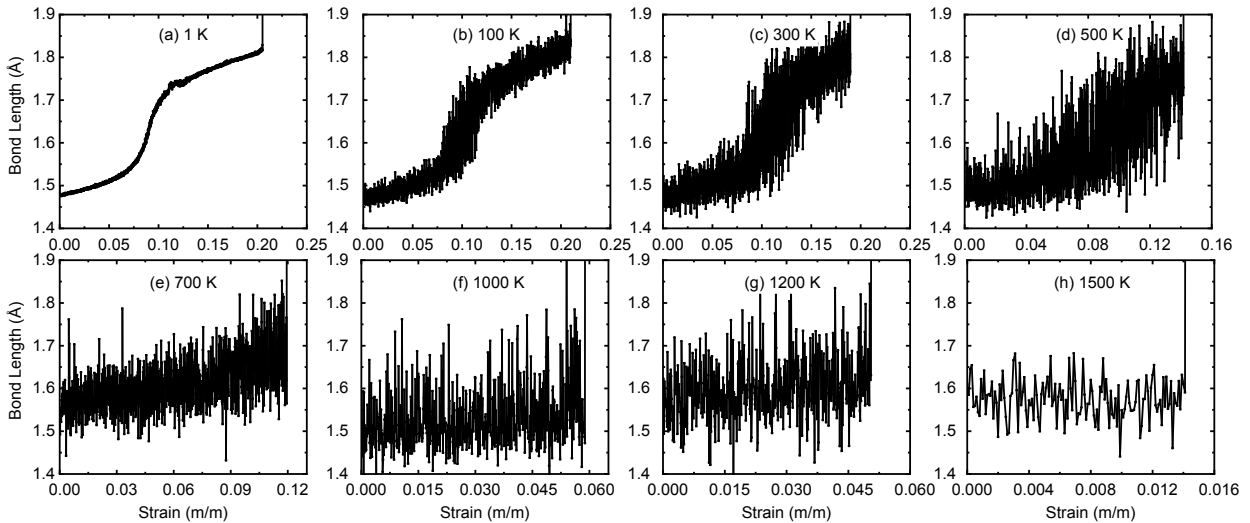


Figure S17 Development of bond length of the skeleton subjected to elongation. (a)-(h) Variation in a localized bond length with globally axial strain for Tube (3,0)_1245 CNNT at temperature from 1-1500 K.

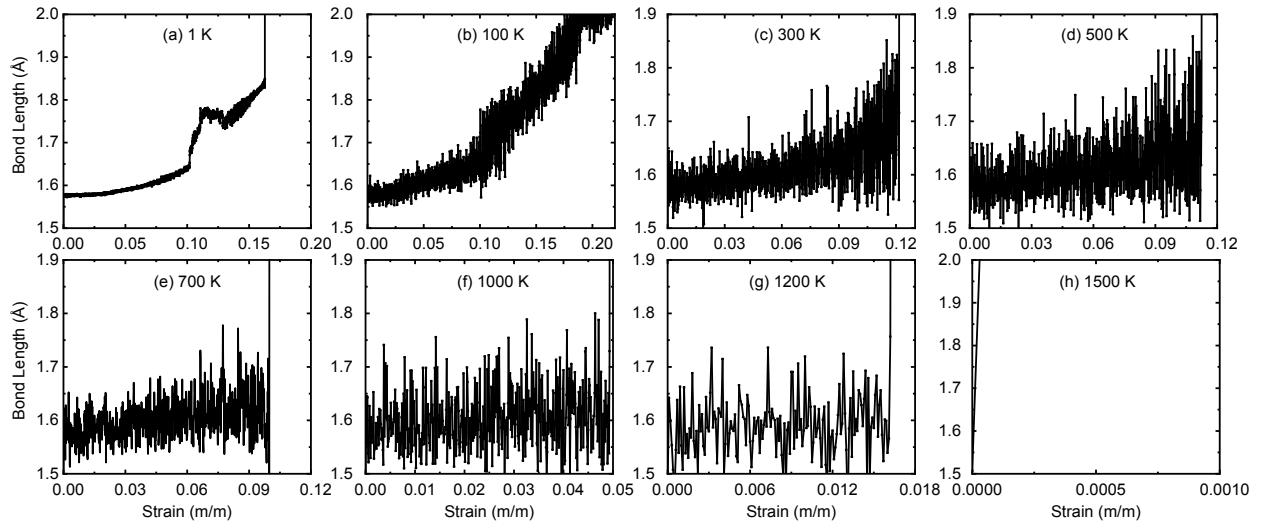


Figure S18 (a)-(h) Variation in a localized bond length with globally axial strain for Polymer I_3-3_25 at temperature from 1-1500 K, respectively.

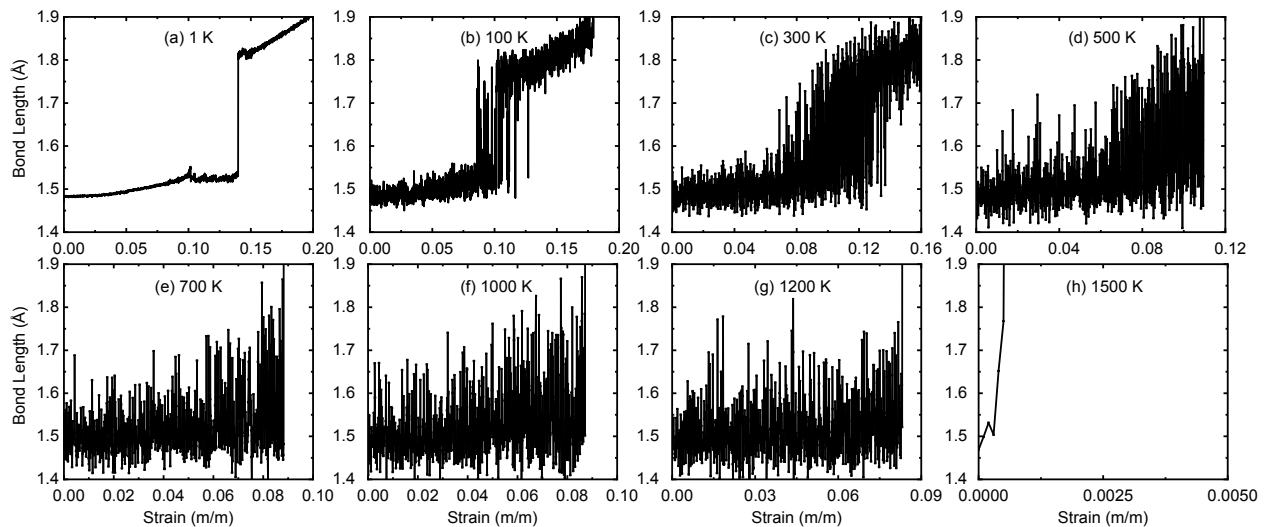


Figure S19 (a)-(h) Variation in a localized bond length with globally axial strain for Polymer I_4-2_36 at temperature from 1-1500 K, respectively.

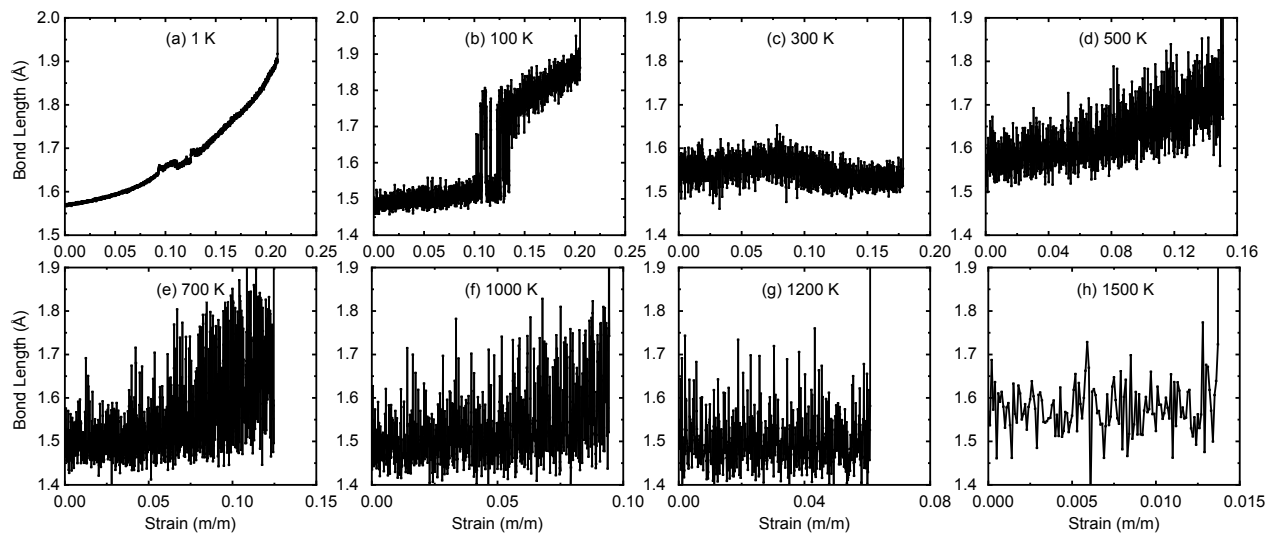


Figure S20 (a)-(h) Variation in a localized bond length with globally axial strain for Polytwistane_153 at temperature from 1-1500 K, respectively.

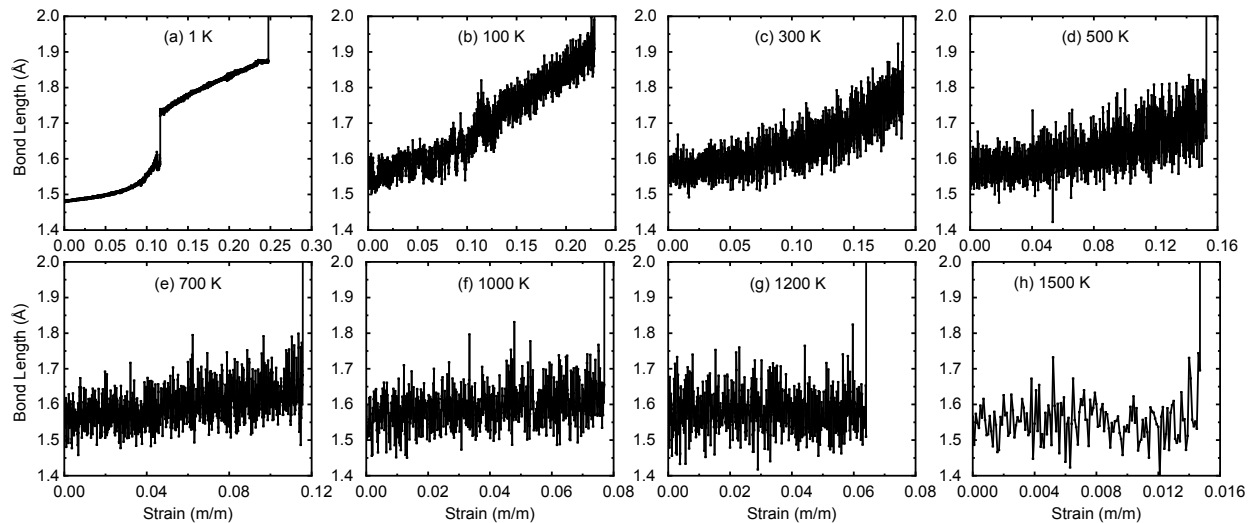


Figure S21 (a)-(h) Variation in a localized bond length with globally axial strain for Tube (3,0)_123456 at temperature from 1-1500 K, respectively.

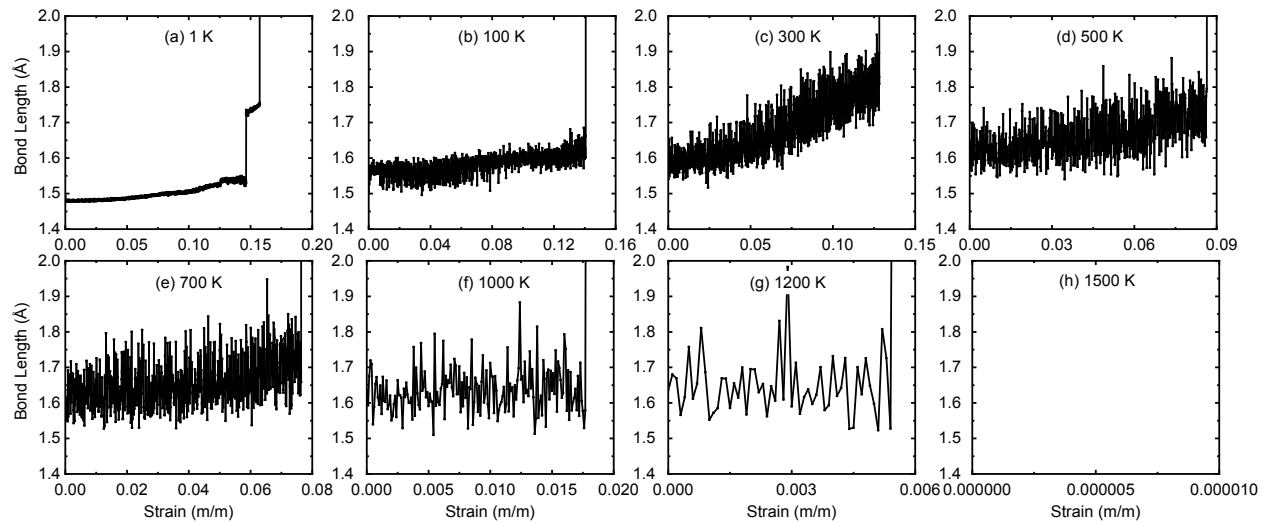


Figure S22 (a)-(h) Variation in a localized bond length with globally axial strain for Zipper polymer_24 at temperature from 1-1500 K, respectively.

References

1. G. Kresse and J. Furthmüller, *Computational materials science*, 1996, **6**, 15-50.
2. K. Glantschnig and C. Ambrosch-Draxl, *New Journal of Physics*, 2010, **12**, 103048.